THE JOURNAL OF PHYSICAL CHEMISTRY A

 VOLUME 109, NUMBER 4, FEBRUARY 3, 2005

ARTICLES

Fast Excited-State Intramolecular Proton Transfer and Subnanosecond Dynamic Stokes Shift of Time-Resolved Fluorescence Spectra of the 5-Methoxysalicylic Acid/Diethyl ether Complex

Mirosława Smoluch, Hem Joshi, Arjen Gerssen, Cees Gooijer, and Gert van der Zwan*

Department of Analytical Chemistry and Applied Spectroscopy, Laser Centre VU, Faculty of Sciences, Vrije Universiteit, De Boelelaan 1083, 1081 HV Amsterdam, The Netherlands

Received: June 8, 2004; In Final Form: November 11, 2004

Excited-state intramolecular proton transfer (ESIPT) occurring in the salicylic acid (SA) derivative 5-methoxysalicylic acid (5-MeOSA) in an apolar solvent (cyclohexane) and in the presence of the hydrogen bond accepting agent diethyl ether (DEE) is investigated. Analysis of the directly measured subnanosecond time-resolved emission spectra (TRES) together with conventional steady-state fluorescence and time-correlated single-photon-counting (TCSPC) decays indicates that ESIPT in this system occurs much faster than fluorescence, and that the equilibrium between normal and tautomeric excited states is established before the emission from both states takes place. However, changes in time- and frequency-resolved fluorescence of the 5-MeOSA/DEE complex are observed due to structural relaxation within the complex, which is reflected in the dynamic Stokes shift of the tautomeric fluorescence band. The normal fluorescence band of 5-MeOSA/DEE does not exhibit marked changes within the investigated time range. A single-exponential relaxation time of 460 ps was determined for the dynamic Stokes shift of the tautomeric band, and it is attributed to a geometric change within the 5-MeOSA/DEE complex upon excitation. Since both tautomeric and normal emission bands are well resolved and exhibit different time-dependent behaviors, a double-well potential appears to be adequate to describe the excited state of the system studied.

1. Introduction

Excited-state intramolecular proton transfer (ESIPT) is one of the fundamental chemical processes. It is believed to be a very fast process that in some cases takes only tens or hundreds of femtoseconds,[1−4] although in certain molecules it also occurs on longer time scales.[5−7] It is generally accepted that several factors determine the rate of ESIPT, such as different atomic motions involved in the process, effects of charge redistribution, and possibly solvent relaxation. In this paper we report the results of a study on the ESIPT process occurring in the salicylic acid (SA) derivative 5-methoxysalicylic acid (5-MeOSA) in an apolar solvent (cyclohexane) and in the presence of the hydrogen bond accepting agent, diethyl ether (DEE).

SA derivatives are well-known to exhibit ESIPT,[8−10] which is usually fast as demonstrated by a single band of large Stokes shift originating from a tautomeric species in steady-state fluorescence spectra.[11] On the other hand, in some SA analogues such as 5-MeOSA, ESIPT is almost completely inhibited and emission occurs prevailingly from the locally excited ("normal") state.[12,13] However, adding DEE to the 5-MeOSA solution in cyclohexane promotes the ESIPT process again so that both the normal band and the tautomeric band show up in the

* Corresponding author. E-mail: zwan@few.vu.nl.

10.1021/jp0475281 CCC: $30.25
Published on Web 01/07/2005

fluorescence emission spectrum.[14] Standard fluorescence decays measured at the maximum wavelengths of both bands differ significantly from each other, and especially a rise time appearing in the long-wavelength decay suggests that the ESIPT process in the 5-MeOSA/DEE complex might be slowed considerably, to occur on the fluorescence lifetime scale.

This observation prompted a more detailed investigation of the time-resolved fluorescence features of 5-MeOSA, using the novel setup built in our laboratory consisting of a state-of-the-art picosecond-gated intensified CCD camera coupled to a spectrograph and a pulsed picosecond Ti−sapphire laser. With this camera it is possible to measure time-resolved emission spectra (TRES) directly on a 100−200 ps time scale with a very good spectral resolution (down to 0.2 nm).[15,16] Thus it was expected that the analysis of the shape and spectral parameters of the recorded TRES would provide additional information on the origin of the wavelength dependence of the fluorescence decays.

2. Experimental Section

5-MeOSA (98%, Aldrich) was purified by crystallization from ethanol. Quinine sulfate (99%, fluorescence indicator, Fluka), DEE (extra pure, VWR International Prolabo), and cyclohexane (spectroscopic grade, Aldrich) were used as received.

Absorption spectra were measured with a Varian Cary 50 Bio UV/vis spectrophotometer. Steady-state fluorescence emission and excitation spectra were recorded with a Perkin-Elmer LS 50B luminescence spectrometer. Fluorescence intensity decays were measured using time-correlated single-photon counting (TCSPC). In the TCSPC setup, a Coherent Mira 900 Ti−sapphire pulse laser (3 ps pulse width) was used as the excitation source. The output of the laser was frequency tripled to obtain the excitation wavelength of 295 nm. Fluorescence was collected with a multichannel-plate photomultiplier (Hamamatsu, R3809U-50), and collected data were recorded with the help of the SPC-630 module (Becker&Hickl GmbH, Berlin, Germany) with a time resolution of about 15 ps. TRES were recorded with the setup consisting of a picosecond-gated intensified CCD camera (La Vision, Göttingen, Germany) coupled to a spectrograph. For excitation the same picosecond Ti−sapphire laser as used with the TCSPC setup was applied and its output was tripled to obtain the excitation wavelength of 291 nm (for technical reasons, for the camera setup it was not possible to obtain enough output from the laser to use the 295 nm wavelength for excitation). The spectra were measured in 50 ps steps over a range of 3 ns using a 300 ps gate time (because of too low fluorescence intensity, the shortest possible gate time of 200 ps could not be employed). Image collection was performed under the control of DaVis software v6.2 (La Vision, Göttingen, Germany).

To determine the instrumental profile (time response) of the TCSPC setup, the excitation light scattered in a silica suspension was recorded. Fluorescence intensity decays were analyzed using Fluofit 3.1 software (PicoQuant GmbH, Berlin, Germany) and were deconvoluted with the instrumental profile. The obtained values of χ^2 were close to 1, indicating a high goodness of fit.

The actual gate time employed in the TRES measurement and the delay time of each measured spectrum were also determined by means of the silica suspension. The wavelength calibration of the spectrometer used in the CCD camera setup was performed using a calibration mercury lamp (Oriel Optics Corporation). Because the spectral range of the 5-MeOSA/DEE emission is very broad, it was not possible to record a full TRES within a single measurement. The full spectral range had to be covered with two different positions of the grating, further on referred to as range 1, 345−530 nm, and range 2, 425−600 nm. The TRES thus obtained were corrected for intensity differences with the use of a fluorescence standard, quinine sulfate, normalized, and then combined to obtain full-range spectra. Following this procedure we could not obtain a satisfactory matching for the spectra below 500 ps; for this reason in the following only the spectra within the range 500−2500 ps will be considered. To be able to determine the TRES for shorter delay times, the procedure must be further optimized, in particular as regards including the deconvolution of the instrumental response (gate time). If the delay times are longer than the gate time, the instrumental response does not influence the recorded spectra and therefore can be neglected. The TRES were analyzed with Origin 7.0 software, using Multi-Peak fit analysis.

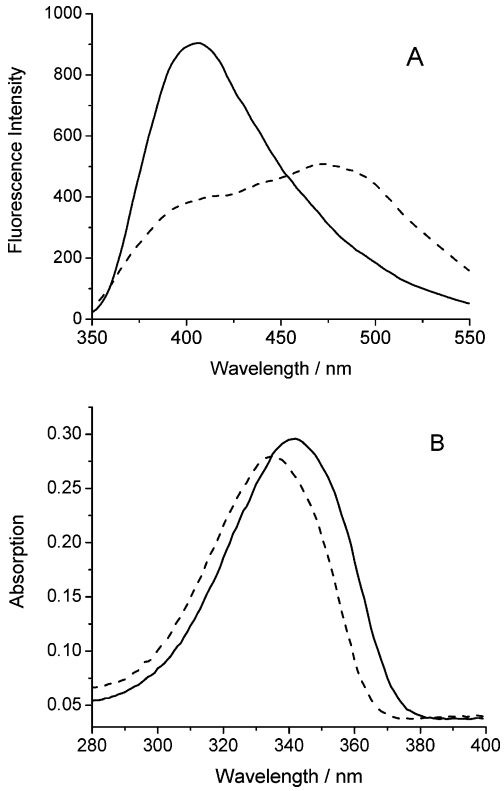

Figure 1. Steady-state fluorescence (A) and absorption spectra (B) of 5-MeOSA in cyclohexane (concentration 3.8×10^{-5} M) with (---) and without (—)1 M DEE. Fluorescence spectra excited at 330 nm (about maximum of absorption), slit 10/10 nm.

3. Results and Discussion

3.1. Influence of DEE on the Steady-State Fluorescence Properties of 5-MeOSA. The fluorescence emission spectrum of 5-MeOSA in cyclohexane excited at its absorption maximum (330 nm) consists of one broad band with the maximum at 400 nm and a long shoulder up to about 600 nm (Figure 1A). Since its mirror image is rather similar to the absorption spectrum (Figure 1), this emission band can be attributed to the excited (normal) form of 5-MeOSA, an assignment in line with results obtained by a fluorescence supersonic jet study.[14] The shoulder observed in the emission spectrum is most probably due to residual ESIPT still occurring in the system (similarly as for 5-methoxysalicylate[13]), an interpretation supported by IR supersonic jet studies reported recently.[17] At the concentrations used in the present study (10^{-6}−10^{-5} M), there is no evidence of

SCHEME 1: Intra- and Intermolecular Hydrogen Bonds in the 5-MeOSA/DEE Complex

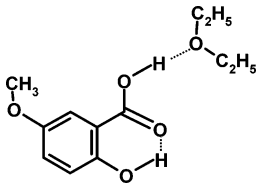

dimers in the steady-state fluorescence spectrum of 5-MeOSA; such dimers were reported for SA.[18] Also, the presence of ground-state rotamers as reported for methyl salicylate can be ruled out in the case of 5-MeOSA.[14]

After the addition of a high concentration (1 M) of diethyl ether (DEE) to the hexane solution, a new band in the 5-MeOSA fluorescence emission spectrum appears with the maximum at about 475 nm; this can be attributed to the enhanced tautomeric emission of 5-MeOSA (Figure 1A). In accordance with this interpretation the short-wavelength normal band is markedly decreased in intensity and its maximum shifted slightly to shorter wavelengths. These changes in fluorescence are accompanied by a blue shift in the absorption spectrum from 342 to 335 nm (Figure 1B). Both effects are consistent with the results already published by Lahmani and Zehnacker-Rentien.[14] They were explained as a specific complexation of 5-MeOSA with DEE which promotes the ESIPT process in 5-MeOSA. This complexation is based on an intermolecular hydrogen bonding (see Scheme 1) which is thought to enhance the acidity of the phenolic proton in 5-MeOSA.

Lahmani and Zehnacker-Rentien did not observe a significant difference between the excitation spectra of 5-MeOSA in cyclohexane (with or without DEE) recorded at 400 and 475 nm, the emission wavelengths of the maxima of both fluorescence bands. In contrast, we observe pronounced differences when excitation spectra are recorded at shorter wavelengths of the emission (blue edge), especially for 5-MeOSA in the presence of DEE (Figure 2A).

The influence of the excitation wavelength on the emission spectrum of the 5-MeOSA/DEE complex appears to be substantial: the ratio of two fluorescence bands is changing continuously upon shifting the excitation wavelength along the whole S_1 absorption band of 5-MeOSA (280−360 nm). Apparently, more normal emission occurs when the complex is excited at shorter wavelengths and more tautomeric emission occurs when the complex is excited at longer wavelengths (Figure 2B). The changes, however, are again most pronounced at the blue edge of the absorption band of 5-MeOSA. The fluorescence spectra of 5-MeOSA without DEE are only slightly dependent on the excitation wavelength, and a shift of the whole spectrum to the blue is observed upon excitation at the blue edge, rather than changes in the spectral shape.

Since the difference in the excitation spectra of 5-MeOSA/DEE complex occurs more at the edge of emission wavelengths than between the two fluorescence bands, we conclude, in agreement with Lahmani and Zehnacker-Rentien, that there is no emission originating directly from excitation of different species in the ground state. Instead, different assemblies in the ground state can be observed which differ in the affinity for undergoing ESIPT after excitation. On the other hand, in the case of 5-MeOSA in pure cyclohexane, following the suggestion of Lahmani and Zehnacker-Rentien, we can assign the changes observed in fluorescence emission and excitation spectra to the presence of two conformational isomers of 5-MeOSA in the ground state which differ in the orientation of methoxy group with respect to the chelate ring (see Scheme 2). Those isomers were detected in the supersonic jet experiment for 5-MeOSA,

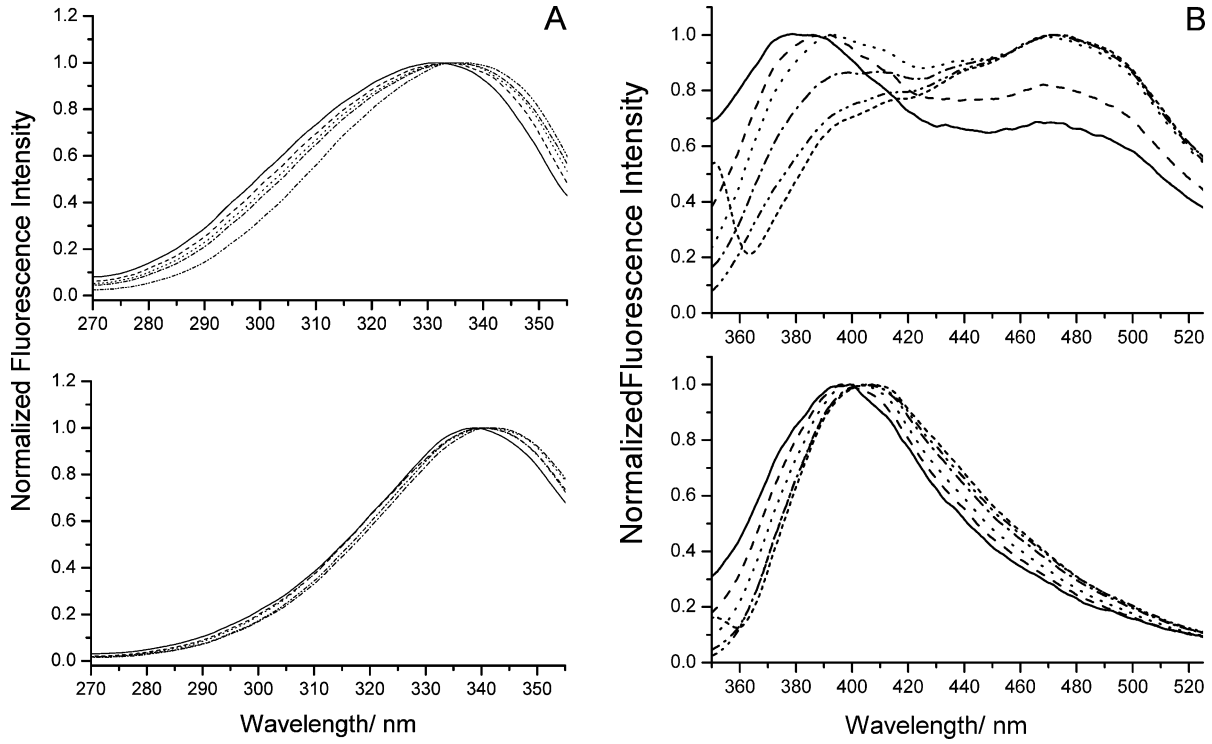

Figure 2. (A) Fluorescence excitation spectra of 5-MeOSA (concentration 3.8×10^{-5} M) in cyclohexane with (upper panel) and without (lower panel) 1 M DEE dependent on emission wavelength: 370 nm (—), 380 nm (---), 390 nm (···), 400 nm (— · —), 500 nm (— ·· —); slit 10/10 nm. (B) Fluorescence emission spectra of 5-MeOSA (concentration 3.8×10^{-5} M) in cyclohexane with (upper panel) and without (lower panel) 1 M DEE, dependent on excitation wavelength: 280 nm (—), 290 nm (— —), 300 nm (···), 310 nm (— · —), 330 nm (— ·· —), 350 nm (- - -); slit 10/10 nm.

SCHEME 2: Two Ground-State Conformational Isomers of 5-MeOSA

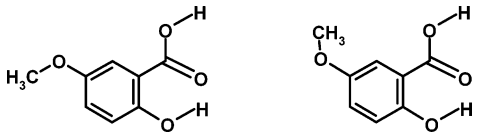

and the energy difference between their S_0-S_1 transitions was identified to be only 272 cm^{-1}. Such a difference, although measured for the gaseous phase, corresponds very well to the shift of a few nanometers in the absorption spectrum around 340 nm in liquid hexane (absorption maximum of 5-MeOSA). The existence of two ground-state isomers can explain the slight wavelength dependence of the excitation and emission spectra of 5-MeOSA in cyclohexane (no DEE) provided that both isomers without DEE have almost identical affinity for undergoing ESIPT. Complexation with DEE might affect the ESIPT affinity of the two isomers to a different extent. Presumably, complexes of different geometry are formed which can be preferentially excited by changing the excitation wavelength; this way the ratio between normal and tautomeric emission will be dependent on the excitation wavelength. A similar effect has been reported for the ESIPT occurring in the complex of a 3-hydroxyflavone derivative with a protein (serum albumin).[19]

3.2. Time-Resolved Fluorescence. To investigate the dynamic aspects of the ESIPT in the 5-MeOSA/DEE complex, fluorescence decays of the sample were measured at the wavelengths where either normal or tautomeric emission is prevailing (i.e., at 400 and 500 nm, respectively). The excitation was performed at 295 nm, so it can be assumed that mostly one of the two 5-MeOSA isomers was excited, i.e., the one possessing higher energy of S_0-S_1 transition and lower affinity to undergo ESIPT.

The analysis of the decays shows some interesting features. They can be fitted very well to two-exponential decay curves (Figure 3). At 400 nm there are two decay components of 480 ps and 2.3 ns, whereas at 500 nm a rise time of 430 ps and a single decay component of 2.4 ns (Table 1) are observed. In contrast, fluorescence of 5-MeOSA in cyclohexane alone does not exhibit a wavelength dependence and decays monoexponentially with the lifetime of 2.1 ns. At first sight these results indicate that the ESIPT process is in competition with fluorescence emission of the normal form of 5-MeOSA in the complex; as a result, it will cause an increase in the fluorescence intensity at the long wavelengths at the expense of the short-wavelength intensity. If this interpretation is correct, the ESIPT process in the 5-MeOSA due to DEE complexation should be considerably slowed to occur on the fluorescence time scale (nanoseconds).

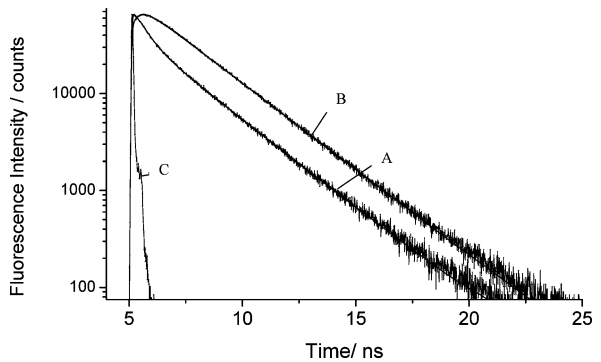

Figure 3. Fluorescence decays of 5-MeOSA/DEE complex in cyclohexane (concentration 2×10^{-6} M) measured with TCSPC technique at different emission wavelengths (two-exponential fits are also shown): 400 (A) and 500 nm (B); instrumental response (C).

TABLE 1: Relaxation Times Obtained for 5-MeOSA/DEE Complex from Exponential Fits to Fluorescence Intensity Decay Traces Measured at Two Different Emission Wavelengths and to the Shift of the TRES Maximum Recorded with the CCD Camera[a]

type of relaxation process	τ_1 [ns]	τ_2 [ns]	α_1	α_2	χ^2
fluorescence intensity decay (TCSPC)					
at 400 nm	0.48	2.3	51.5	48.5	1.04
at 500 nm	0.43	2.4	−5.3	14.4	1.09
shift of TRES maximum (CCD camera)					
spectra as measured	0.47				0.998
calibrated and combined spectra	0.46				0.97

[a] τ_1, τ_2, relaxation times; α_1, α_2, amplitudes corresponding to each relaxation time (for biexponential relaxation); χ^2, goodness of fit.

To verify this assumption, time-resolved emission spectra of the 5-MeOSA/DEE complex were recorded directly with the use of the fast-gated CCD camera setup. In Figure 4A it is very clear that TRES recorded at 500 ps up to 2500 ps after excitation exhibit a red shift and a pronounced change of the spectral shape for the 5-MeOSA/DEE complex, whereas for 5-MeOSA alone the TRES appear to be identical. The changes in the TRES of the complex are consistent with the wavelength dependence of fluorescence decays: in both cases a significant decrease of short-wavelength fluorescence and a simultaneous comparatively smaller increase of long-wavelength fluorescence are observed. There is a small discrepancy in the maximum wavelengths between the TRES and the steady-state spectra, but since it does not influence the view on the dynamic properties of our system, it can be neglected for the purpose of this study.

TRES of 5-MeOSA were fitted well to double-Gaussian functions both with and without DEE (Figure 4B,C). The resulting higher energy Gaussian bands have almost the same maximum wavenumber for both samples (ca. 24 000 cm^{-1}), while for the 5-MeOSA/DEE complex the maximum is slightly shifting to the red in time. In contrast, the lower energy band for the complex is positioned much more to the red compared to 5-MeOSA alone and additionally it is continuously shifting to the red over the whole delay-time range analyzed (the obtained maximum wavenumbers being 21 000 cm^{-1} for 5-MeOSA alone and between 20 700 and 20 000 cm^{-1} for the complex). On the basis of the steady-state fluorescence studies, the two Gaussians can be assigned to the two bands building up the total fluorescence spectrum of 5-MeOSA (with or without DEE) indicated as the locally excited (normal) and the tautomeric band, respectively.

Assuming that the two Gaussians resulting from the fits represent the normal and the tautomeric emission and the ESIPT process is still proceeding in the system, the relative area of the bands should change with time since the tautomeric emission should increase at the expense of the normal emission. Figure 5A shows that this is not observed in the system studied. Although the plot of the ratio of the normal and tautomeric band areas exhibits a large error due to the noise of the TRES (introduced additionally by the calibrating and combining procedure; see the Experimental Section), it is obviously constant in time within the range studied (500−2500 ps), indicating an equilibrium between normal and tautomeric species in the excited state. On the other hand, an unambiguous shift of the maximum of the tautomer band to the red can be observed in contrast to a hardly detectable shift of the normal band (see Figure 5B).

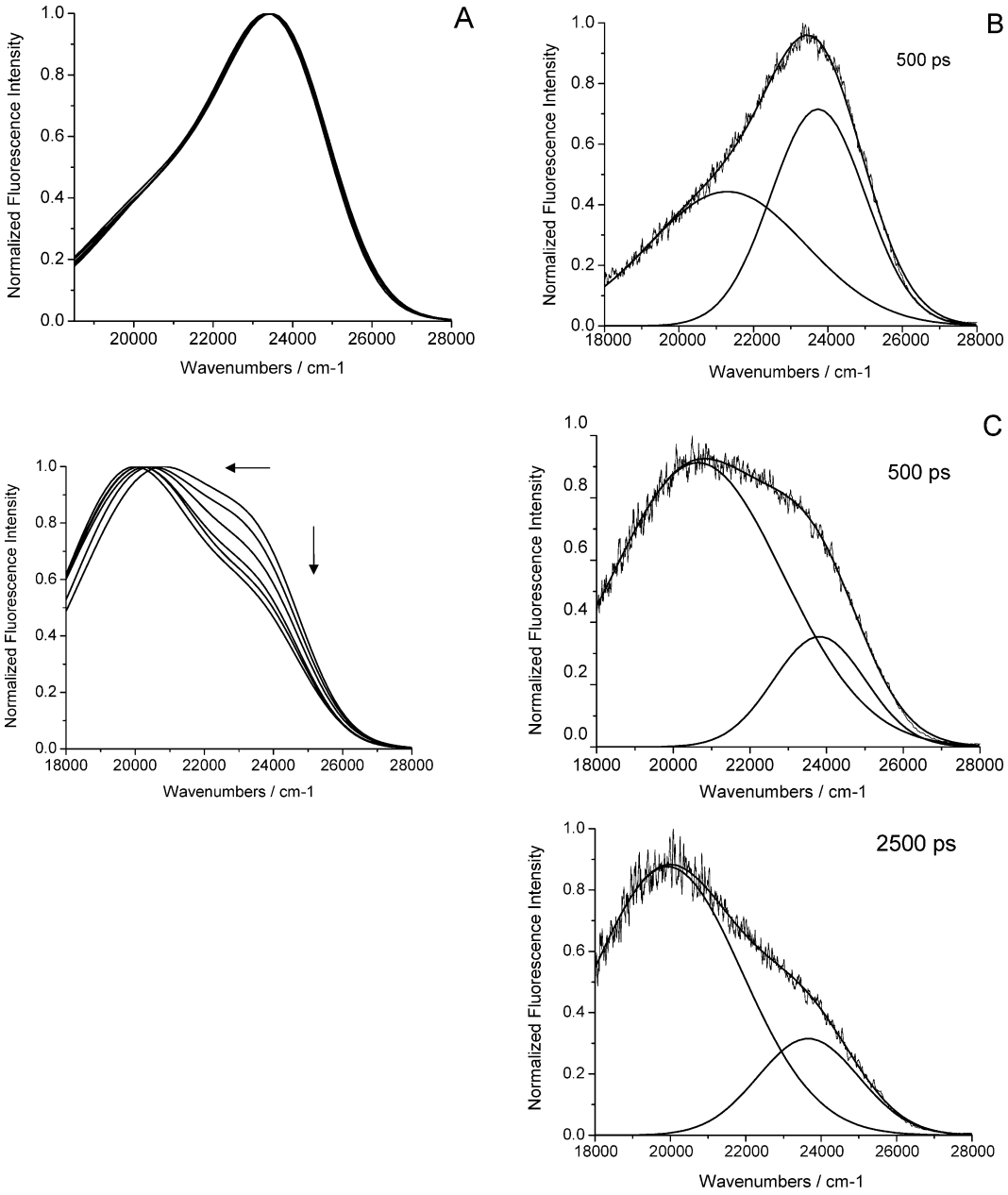

Figure 4. Results of Gaussian fits to TRES of 5-MeOSA with and without DEE. (A) Total fitted curves. Upper panel: 5-MeOSA in cyclohexane; lower panel: 5-MeOSA/DEE complex; delay times 500, 700, 1000, 1500, 2000 ps, 2500 ± 150 ps (arrows indicate the changes in spectra with time). (B) Two Gaussian bands resulting from the fit for 5-MeOSA in cyclohexane (identical for all delay times). (C) Two Gaussian bands resulting from the fit for the 5-MeOSA/DEE complex for different delay times.

The above results for the TRES of the complex strongly suggest that the large changes of the spectral shape and the red shift of the total spectrum are not caused by ESIPT competing with fluorescence decay. Instead, the changes should be attributed to a Stokes shift of tautomeric 5-MeOSA due to the complexation with DEE. The origin of this dynamic Stokes shift is most probably the change of geometry within the complex adjusting to the new charge distribution and geometry of 5-MeOSA molecule after excitation. Apparently, this geometric relaxation of the complex in the excited state affects considerably the energy of the tautomeric state of 5-MeOSA; the energy change for the normal band is almost negligible.

An alternative mechanism, known in the literature as preferential solvation,[20−22] could also be considered to explain a nanosecond dynamic Stokes shift of 5-MeOSA fluorescence in the mixture of two solvents of different polarities (cyclohexane and DEE, although these differ little in dielectric constant). However, the maximum of the steady-state fluorescence band of 5-MeOSA does not depend on the molar fraction of DEE down to 0.002 M; already at that value the maximal Stokes shift is obtained. These results suggest that preferential solvation is not involved in the observed dynamic Stokes shift and additionally support the hypothesis of complexation between 5-MeOSA and DEE.

To avoid the uncertainties introduced to the TRES by the calibration and combining procedure, the analysis of uncorrected and uncombined spectra of 5-MeOSA/DEE complex in range 2 (425−600 nm; see the Experimental Section) was carried out separately. For this purpose it was assumed that in this spectral region the emission from the locally excited state of 5-MeOSA/DEE complex does not show up, so almost purely tautomeric emission is observed. The uncorrected spectra of range 2 for 5-MeOSA/DEE were appropriately fitted to a single-Gaussian curve (the values of R^2 for all spectra were 0.97−

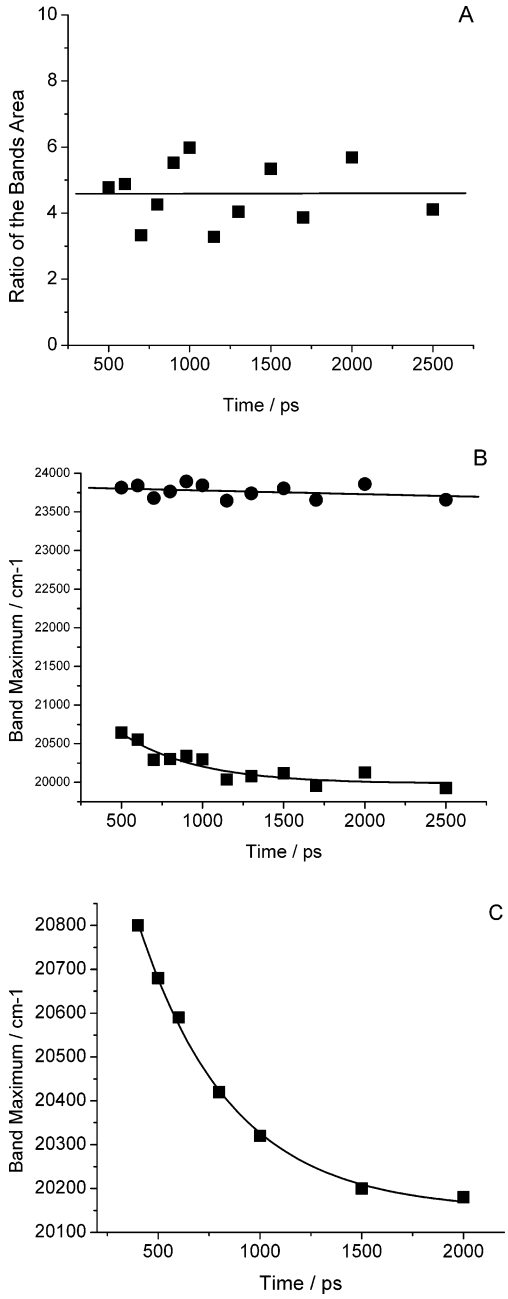

Figure 5. Results of analysis of Gaussian peak parameters obtained for TRES of 5-MeOSA with DEE. (A) Ratio of area of tautomeric and normal bands versus time. (B) Maximum wavenumbers of tautomeric (■) and normal (●) bands versus time (based on Gaussian fits to calibrated and combined TRES). (C) Maximum wavenumbers of tautomeric band versus time (based on Gaussian fits to TRES as measured).

0.99), which confirms the above assumption. The maximum wavenumbers of the fitted spectra were plotted as a function of time and fitted quite nicely ($R^2 = 0.998$) with the single-exponential decay curve (Figure 5C). The relaxation time obtained from this fit (460 ± 30 ps) is in excellent agreement with the short decay components obtained for the 5-MeOSA/DEE complex: 480 ± 50 ps for the decay at 400 nm and 430 ± 50 ps for the rise time at 500 nm (see Table 1). This good agreement strongly suggests that the changes observed in the decays are solely due to the dynamic Stokes shift of the tautomeric fluorescence band of 5-MeOSA caused by structural relaxation of the complex. Thus, there is no other detectable process occurring on the fluorescence time scale. A very similar value of the relaxation time, but less precise (470 ± 160 ps), was also determined by the single-exponential fit of the maximum wavenumbers obtained from the analysis of the full TRES of the 5-MeOSA/DEE complex plotted against time (see Figure 5B).

Apparently the slow geometric relaxation in 5-MeOSA/DEE system excited at the blue edge of absorption is well described by a single relaxation time, which suggests that predominantly one of two types of the complex (one of two ground-state isomers of 5-MeOSA) is excited. A single relaxation time also indicates a dominating effect responsible for geometric relaxation of 5-MeOSA in the complex.

The ESIPT process in 5-MeOSA, both with and without DEE, apparently still occurs much faster than the fluorescence emission. The equilibrium between normal and tautomeric species in the excited state is already established before the emission takes place: all the analyzed TRES of 5-MeOSA in pure cyclohexane and in the complex with DEE contain both the tautomeric emission and normal emission at a constant ratio. Also, except for the geometric relaxation component, only one decay time (ca. 2 ns) was determined in fluorescence decays of 5-MeOSA both with and without DEE. If ESIPT in this system was not much faster than fluorescence, two different decay times would be expected for normal and tautomeric emission. Kinetic considerations based on a simple model supporting this assumption are presented in the Appendix.

4. Conclusions

The detailed analysis of conventional steady-state and time-resolved fluorescence data together with the information provided by the directly measured TRES suggests that in the 5-MeOSA/DEE complex ESIPT still occurs much faster than fluorescence emission. Since both tautomeric emission and normal emission are present in time-resolved fluorescence spectra in the same relative amount, the equilibrium between normal and tautomeric forms in the excited state is established before emission takes place. Also, the equality of the fluorescence lifetimes of both species indicates that the ESIPT process in the studied system occurs much faster than fluorescence.

The classical double-well potential description of the excited-state proton coordinate appears to be valid for 5-MeOSA in complex with DEE because two distinct emission bands are observed in both steady-state and time-resolved fluorescence spectra. It is further supported by the fact that both normal and tautomeric bands (and thus both excited states, respectively) of 5-MeOSA appear to be influenced in a different way by the geometric relaxation of the complex. Also, two distinct bands can be well distinguished in the TRES of 5-MeOSA in pure cyclohexane (see Figure 4B), which is in contrast to a barrierless transition in 5-MeOSA suggested by previous authors based on the results of supersonic jet study.[14]

The above results also indicate that the Stokes shift of the tautomeric excited state of 5-MeOSA has a slow component due to the geometric relaxation within the complex with DEE and thus occurs on the fluorescence lifetime scale. A single relaxation time of 460 ps was determined for this process, which suggests that it is dominated by one type of effect.

Thus, the influence of DEE on the ESIPT in 5-MeOSA appears to be 2-fold: it shifts the ESIPT equilibrium markedly in the excited state toward the tautomeric form of 5-MeOSA and furthermore slows the Stokes shift of the tautomeric emission band due to the geometric rearrangement within the complex upon excitation.

The high-resolution TRES of the system directly recorded with the CCD camera appear to be a convenient tool to unravel the dynamics of subnanosecond processes in the excited state, which manifest themselves via changes in a total time- and frequency-resolved emission profile. Further development of the data analysis is in progress; it should enable investigation of the processes occurring on a shorter, 50−200 ps, time scale, particularly the early TRES recorded for 5-MeOSA in pure cyclohexane.

5. Appendix

In this appendix we give a brief derivation of the fact that fluorescence rates for the different (normal and tautomeric) forms are the same if equilibration in the excited state is fast. We assume that the normal "N" form is initially excited, and can either decay to the ground state or be transformed to the "T" state. The number of excited N molecules, n_N, as a function of time is therefore determined by

$$\frac{dn_N(t)}{dt} = -(k_N + k_f)n_N(t) + k_r n_T(t) \tag{1}$$

where k_N is the direct decay rate to the ground state, comprising both fluorescence and nonradiative processes, k_f is the forward rate for ESIPT, and k_r is the rate with which the tautomer can be back-converted to the normal form. Similarly we have for the number of T molecules, n_T, in the excited state:

$$\frac{dn_T(t)}{dt} = -(k_T + k_r)n_T(t) + k_f n_N(t) \tag{2}$$

where k_T is the rate with which the tautomer is converted to the ground state. This linear system of equations can of course be solved for any initial conditions, but for the purpose of this paper we are only interested in the eigenvalues of the decay matrix, which are found to be:[11]

$$\lambda_{1,2} = \frac{1}{2}[k_N + k_f + k_T + k_r \pm \sqrt{(k_N + k_f - k_T - k_r)^2 + 4k_f k_r}] \tag{3}$$

In general, this leads to two decay times for both the normal and the tautomeric forms, one of which corresponds to an ingrowth for the tautomer. Note that, if the reverse rate $k_r = 0$, the species decay with rates $k_N + k_f$ and k_T, respectively, and it would be extremely coincidental if these were the same for both forms.

In the main body of the article we argue that the ingrowth of the tautomer is actually related to a spectral shift, and not related to the ESIPT reaction. If we assume that the ESIPT reaction is still very fast, we can expand both eigenvalues in $1/k_f$, and we find that decay is governed by two rates: the equilibration rate in the excited state

$$\lambda_1 \approx k_f + k_r \tag{4}$$

and the decay rate of both excited states:

$$\lambda_2 \approx \frac{k_N + K_{eq}^* k_T}{1 + K_{eq}^*} \tag{5}$$

where

$$K_{eq}^* = k_f/k_r \tag{6}$$

is the equilibrium constant in the excited state.

Unfortunately it is impossible, because we do not have access to the tautomer in the ground state, to actually calculate the excited-state equilibrium constant from our data.

References and Notes

(1) Schwartz, B. J.; Peteanu, L. A.; Harris, C. B. *J. Phys. Chem.* **1992**, *96*, 3591.
(2) Herek, J. L.; Pedersen, S.; Banares, L.; Zewail, A. H. *J. Chem. Phys.* **1992**, *97*, 9046.
(3) Ameer-Beg, S.; Ormson, S. M.; Brown, R. G.; Matousek, P.; Towrie, M.; Nibbering, E. T. J.; Foggi, P.; Neuwahl, V. R. *J. Phys. Chem. A* **2001**, *105*, 3709.
(4) Bader, A. N.; Ariese, F.; Gooijer, C. *J. Phys. Chem. A* **2002**, *106*, 2844.
(5) Swinney, T. C.; Kelley, D. F. *J. Chem. Phys.* **1993**, *99*, 211.
(6) Shynkar, V. V.; Mely, Y.; Duportail, G.; Piemont, E.; Klymchenko, A. S.; Demchenko, A. P. *J. Phys. Chem. A* **2003**, *107*, 9522.
(7) Bader, A. N.; Pivovarenko, V.; Demchenko, A. P.; Ariese, F.; Gooijer, C. *Spectrochim. Acta A* **2003**, *59*, 1593.
(8) Le Gourrierec, D.; Ormson, S. M.; Brown, R. G. *Prog. React. Kinet.* **1994**, *19*, 211.
(9) Joshi, H. C.; Mishra, H.; Tripathi, H. B. *J. Photochem. Photobiol. A* **1997**, *105*, 15.
(10) Arnaut, L. G.; Formosinho, S. J. *J. Photochem. Photobiol. A* **1993**, *75*, 21.
(11) Joshi, H. C.; Gooijer, C.; van der Zwan, G. *J. Phys. Chem. A* **2002**, *106*, 11422.
(12) Joshi, H. C.; Gooijer, C.; van der Zwan, G. *J. Fluoresc.* **2003**, *13*, 227.
(13) Acuna, A. U.; Toribio, F.; Amat-Guerri, F.; Catalan, J. *J. Photochem.* **1985**, *30*, 339.
(14) Lamahni, F.; Zehnacker-Rentien, A. *J. Phys. Chem. A* **1997**, *101*, 6141.
(15) Stortelder, A.; Buijs, J. B.; Bulthuis, J.; Gooijer, C.; van der Zwan, G. *Appl. Spectrosc.* **2004**, *58*, 705.
(16) Stortelder, A.; Buijs, J. B.; Bulthuis, J.; van der Vies, S. M.; Gooijer, C.; van der Zwan, G. *J. Photochem. Photobiol. B* **2004**, *78*, 53.
(17) El-Nasr, E. A. E.-H. A.; Fujii, A.; Ebata, T.; Mikami, N. *Chem. Phys. Lett.* **2003**, *376*, 788.
(18) Joshi, H. C.; Tripathi, H. B.; Pant, T. C.; Pant, D. D. *Chem. Phys. Lett.* **1990**, *173*, 83.
(19) Demchenko, A. P. *Biochim. Biophys. Acta* **1994**, *1209*, 149.
(20) Molotsky, T.; Huppert, D. *J. Phys. Chem. A* **2002**, *106*, 8525.
(21) Agmon, N. *J. Phys. Chem. A* **2002**, *106*, 7256.
(22) Van, S.-P.; Hammond, G. S. *J. Am. Chem. Soc.* **1978**, *78*, 3895.